Physicochem. Probl. Miner. Process. 53(2), 2017, 920−942

www.minproc.pwr.wroc.pl/journal/

Physicochemical Problems of Mineral Processing

ISSN 1643-1049 (print)
ISSN 2084-4735 (online)

Received August 15, 2016; reviewed; accepted December 2, 2016

Effective parameters on generation of nanobubbles by cavitation method for froth flotation applications

Ziaeddin Pourkarimi[*], Bahram Rezai[*], Mohammad Noaparast[**]

[*] Department of Mining and Metallurgical Engineering, Amirkabir University of Technology (Tehran Polytechnics), Tehran, Iran. Corresponding author: rezai@aut.ac.ir (Bahram Rezai)
[**] School of Mining Engineering, University of Tehran, Tehran, Iran

Abstract: The significant recovery increase in flotation of fine particles using nanobubbles has been one of the major topics in flotation science in recent years. Fine bubbles have an important effect on gas hold-up, which is necessary in froth flotation of minerals based on the process industries. At a given gas hold-up, using finer bubbles can reduce frother consumption. An exclusive nanobubble generation system has been developed in Iran Mineral Processing Research Center (IMPRC) to evaluate the effect of nanobubbles on the froth flotation performance. This device, which enhanced venturi tubes, works according to cavitation phenomena. The venturi tube is the most widely used hydrodynamic cavitation device, in which liquid flow increases in the conical convergent zone of the tube due to the thin diameter. The liquid in the cylindrical throat is higher in a flow velocity and lower in a pressure than the liquid in the entrance cylinder, which results in cavitation. In this research work, various factors such as the frother type and dosage, pH, compressed air flow, pressure in cavitation nozzle, gas types, temperature and venturi tube internal diameter were studied. For this purpose, a five-level central composite experimental design was used to check the influence of four important parameters on the median size and volume of nanobubbles. Online measurement of the bubbles size was implemented by a laser particle size analyzer (LPSA), according to standard BS ISO 13320-09. Due to the above parameters and obtained responses, the analysis of variance (ANOVA) was conducted with a suitable model to optimize the conditions, with the aim of minimizing the size of air bubbles. The optimal conditions were: frother (MIBC) dosage of 75.8 mg/dm^3, air flow rate of 0.28 dm^3/min, pressure of 324 kPa and pH of 9.5. The median bubble size d_{50} was equal to 203 nm. To validate the results, a test under optimum conditions was performed and the obtained results indicated that there was a good fit at the confidence interval of 95% and reflected the repeatability of the process.

Keywords: *flotation, nanobubble, cavitation, venturi, laser particle size analyzer*

Introduction

Flotation of fine particles has long been a focus of researchers in the area of mineral processing. One of the significant methods, particularly in recent years, is using nanobubbles simultaneously along with the typical bubbles during flotation. Hence,

http://dx.doi.org/10.5277/ppmp170220

generation of nanobubbles with proper stability as well as scale-up capability is the major technological challenge in the flotation technology.

Generation of nanobubbles in froth flotation is a versatile and extremely complex physicochemical process. Several variables affect nanobubble generation. The role of water vapour and other gases within cavity bubbles in particle-bubble attachment remains to be explored, as does the action of frother. Embedding hydro-dynamic cavitation into flotation systems to take advantage of its unique features is expected to develop the next generation of flotation machines.

Hampton and Nguyen (2010) found that the effect of nanobubbles on flotation of coal in saline environments was important due to changes of the surface characteristics of the mineral species. Fan and Tao (2008) applied this technique for flotation of large and ultrafine particles of coal and phosphate. Furthermore, Sobhy and Tao (2013) used nanobubbles in flotation of fine particles of coal. Ahmadi et al. (2014) used nanobubbles for flotation of fine particles of pure chalcopyrite. Zhang and Seddon (2016) focused on interactions of nanobubble and gold nanoparticles in bulk solutions. They found that, unlike conventional froth flotation, where bubble–particle interactions were driven mainly through collisions, for bulk nanobubble solutions the principle interaction was through nucleation of new nanobubbles on particles.

In the present study, nanobubble generation was carried out via a specially designed cavitation tube at varying values of eight major parameters, that is frother type and dosage, pressure in cavitation tube nozzle, venturi tube diameter, pH of solution, various gas types, temperature and dissolved air flow rate. The major purpose of this study was to evaluate the selectivity and repeatability of the process and to optimize parameters that have an effect on the size of bubbles.

Cavitation is formation and simultaneous collapse of vapour cavities in a liquid. It usually occurs when a liquid is subjected to rapid changes of pressure that cause formation of cavities where the pressure is relatively low. When subjected to higher pressure, the voids implode and can generate an intense shock wave (Zhou et al., 1994).

There are various kinds of cavitation, which are classified in Fig. 1. This study particularly focused on hydrodynamic cavitation. Hydrodynamic cavitation describes the process of vaporisation, bubble generation and implosion, which occur in a flowing liquid as a result of decrease and subsequent increase in the local pressure.

Hydrodynamic cavitation is well described by Bernoulli's equation:

$$P + \frac{1}{2}\rho U^2 = C \text{ (constant)} \tag{1}$$

where U is the water flow velocity at a point, P is the pressure, and ρ is the liquid density. Rearranging Equation (1) gives:

$$U^2 + \frac{2P}{\rho} = \frac{2C}{\rho}. \tag{2}$$

It indicates that the pressure is negative when the water flow velocity U exceeds $\sqrt{\frac{2C}{\rho}}$. Figure 2 shows the mechanism of nanobubble generation in the venturi tube.

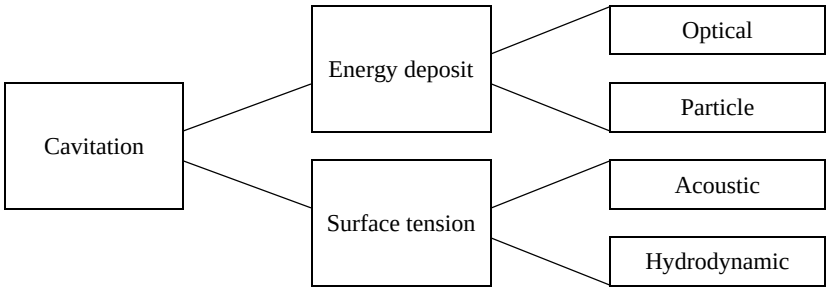

Fig. 1. Classification of cavitation based on the mechanism of bubble generation (Li, 2001)

Hydrodynamic cavitation does not occur during direct streams. In a simple stream without splits and turbulence, changes in flow direction and convergence, can cause cavitation. In order to measure the flow resistance versus cavitation, the cavitation number (K_c) is defined:

$$K_C = \frac{P_{loc} - P_{vap}}{\frac{1}{2}\rho_1 U_{loc}^2} \tag{3}$$

where P_{loc} is the ambient pressure, U_{loc} is the velocity of stream and P_{vap} is the pressure of vapor. Cavitation takes place when K_c is either equal to the initial cavitation number (K_i) or less than it, which is obtained from laboratory results (generally K_i<3, by decreasing cavitation number, due to static pressure decrease or the stream velocity increase, cavitation will increase) (Zhou et al., 1994).

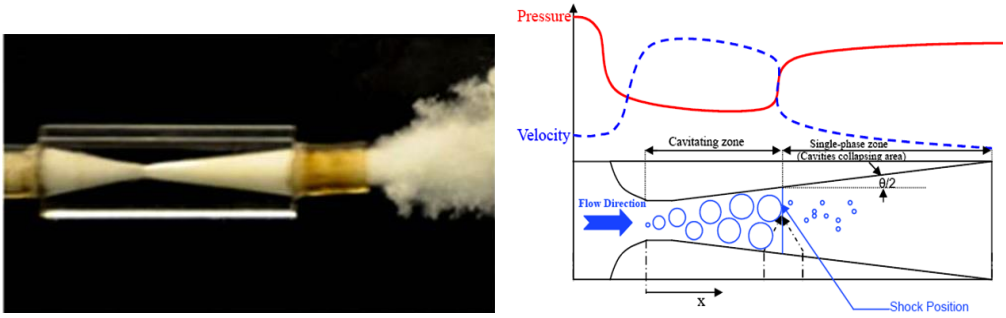

Fig. 2. Mechanism of nanobubble generation in the venturi tube (Sayadi, 2007)

Figure 3 shows the effect of nanobubbles on the coarse and fine particles to attach conventional bubbles. As shown in Fig. 3, the advantage of the cavitation venturi tube-generated picobubbles and nanobubbles, incorporated with conventional-sized bubbles

such as micro-bubbles, in flotation, has been explained by two factors that contribute to the increased flotation rate constant: *i*) picobubbles and nanobubbles formed insitu on hydrophobic particle surfaces may cause aggregation by a bubble-bridging mechanism, resulting in increased collision probability with the bubbles; *ii*) particles frosted with pico-nanobubbles may present a surface favourable for attachment to conventional flotation sized bubbles (Tao, 2004; Zhou et al., 2009).

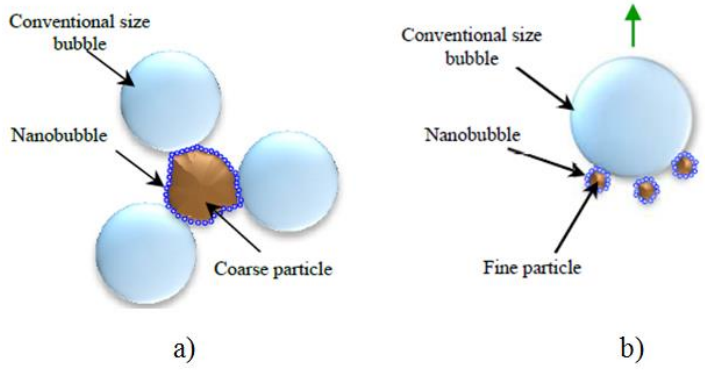

Fig. 3. Effect of nanobubble attachment to conventional bubbles, a) coarse particle, b) fine particle (Fan and Tao, 2008)

Materials and methods

Materials

Several frothers such as MIBC (Methyl Isobutyl Carbinol), Aero65 which is propylene glycol, Pine 90 which is a modified version of pine oil, PEB 70 (alcohol based frother), Flo-Y-S (mixed fatty acid) and Apirole, which are modified collector-frother for phosphate processing, were used in this study. Most of these surfactants were produced in Isfahan Copolymer Company, Iran. Moreover, various gas types such as argon, nitrogen, oxygen, carbon dioxide and filtered compressed air were employed in this research work.

Methods

Generation of nanobubbles was performed based on the cavitation phenomenon through static mixers and venturi tubes. For this purpose, a particular device, which was produced and developed at IMPRC (Iran Mineral Processing Research Center), was applied. Schematic setup of the nanobubble generating and sampling system to measure the bubble size and volume is presented in Fig. 4. Online measurement of the bubbles size was implemented by a laser particle size analyser (LPSA), according to standard BS ISO 13320_09. A Malvern mastersizer 2000 LPSA was used for measuring the size distribution and volume of the bubbles.

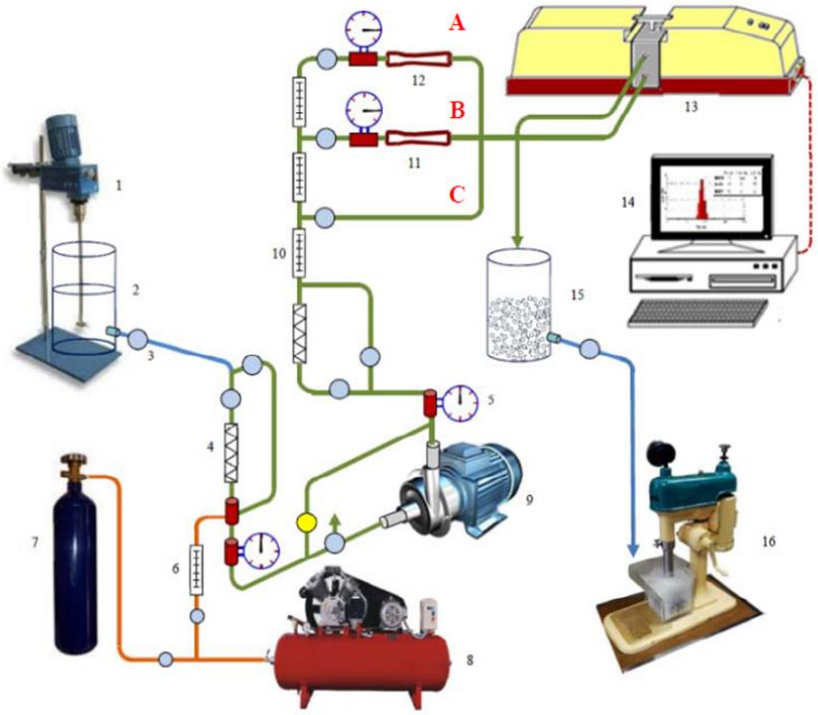

1. agitator, 2. conditioning tank, 3. valve, 4.static mixer, 5. pressure meter, 6. manometer, 7. gas capsule, 8.air compressor, 9. pump, 10. water flow meter, 11. venturi tube (d = 1.5 mm), 12. venturi tube (d = 2.2 mm), 13. laser particle size analyzer (LPSA), 14. computer, 15. nanobubble tank, 16. Denver flotation cell

Fig. 4. Schematic setup of laser particle size analyzer and bubble system for nanobubble size measurement

As it is shown in Fig. 4, the identified frother could be added into the tank (#2) and after appropriate conditioning time, because of the suction that is resulted by the centrifugal pump (#9), the solution is sent to the venturi tubes (destination *A* and *B*) among static mixers. The point where the velocity of stream comes down and the pressure goes up suddenly results in hydrodynamic cavitation phenomena that leads to nanobubbles generation. It is clear that destination *C* is a bypass that allows evaluating the effect of static mixers on the absence of venturi tubes. The venturi tube inlet pressure of the solution as well as compressed air flow is adjustable. The compressed air or specified gas can be added to the solution before entering the pump. Static mixers cause the gas to effectively mix in the solution. The solution containing nanobubbles is transferred to the laser particle size analyzer (#13) through pump (#9) propulsion for online measurement of bubble size according to standard BS ISO 13320_09. Figure 5 shows a comprehensive image from the applied venturi tube in this research.

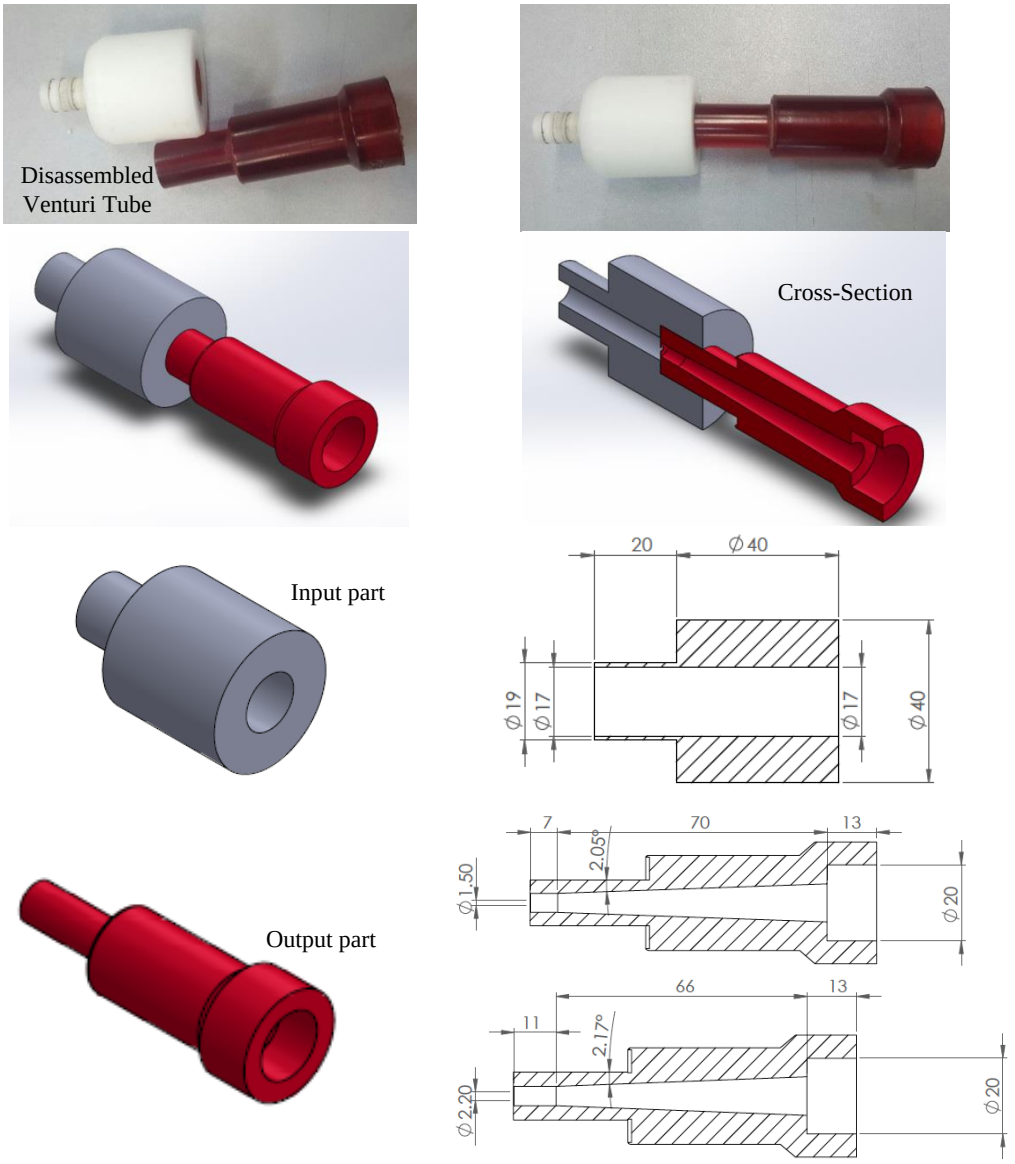

Fig. 5. Venturi tube that is applied in this research and the cross-section of its various parts

In this research, nanobubble generation was carried out with changing values of eight major parameters, that is frother type and dosage, pressure in cavitation tube nozzle, venturi tube diameter, pH of solution, various gas types, temperature and dissolved air flow rate. The main purpose of this study was to evaluate the selectivity and repeatability of the process, and optimization parameters which are effective on the bubbles size.

Results and discussion

Figures 6-11 present the effect of various parameters which are effective on the size of bubbles. It was found that with increasing the dissolved air flow rate and size of bubbles the specific values of the other studied parameters decreased. In addition, the decreasing trend of bubble size with pressure increase is shown in Fig. 4. Also, the decreasing the venturi diameter caused the bubble size decrease. Furthermore, frother concentration increment could cause the bubbles to be finer. However, generated nanobubbles in the presence of Flo-Y-S as a frother were significantly smaller than those produced by MIBC.

Venturi tube diameter

The Venturi internal diameter is one of main parameters having an influence on the bubble size. In this study, two venturi tubes with different entrance diameters of 2.2 mm and 1.5 mm were used to compare the results. As expected, in the case where other parameters were kept constant, bubbles produced by the 2.2 mm diameter venturi tube were larger than the 1.5 mm one. Theoretically, it can be stated that venturi tubes with smaller diameter lead to higher pressure versus the larger ones. In this case, cavitation causes a reverse velocity decrease, little more than larger diameter venturi. On the other hand, smaller bubble diameters are resulted by decreasing the venturi internal diameter. This means that the venturi internal diameter increment has a direct effect on the reduction of bubble size. Figure 6 shows this comparison based on the measured data.

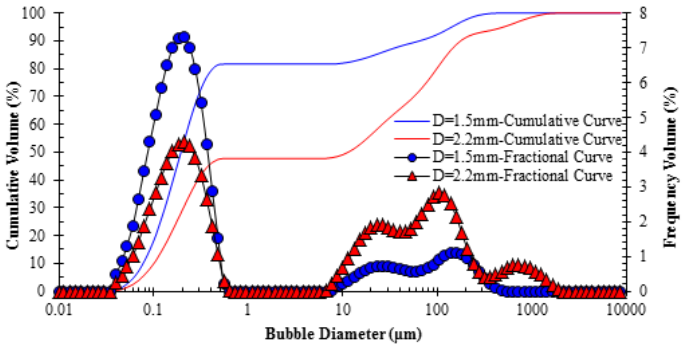

Fig. 6. Influence of venturi tube diameter on size distribution of bubbles

Frother type

Various types of frothers such as: MIBC, Aero65, Pine 90, PEB 70, Flo-Y-S and Apirole were used for generation of bubbles. Based on the results obtained from different experiments, the median size of nanobubbles for various frothers was obtained in accordance with the order:

$$Db(0.5)_{\text{Pine 90}} < Db(0.5)_{\text{Apirole}} < Db(0.5)_{\text{A65}} < Db(0.5)_{MIBC} < Db(0.5)_{PEB\ 70}. \quad (4)$$

The size reduction of bubbles in the presence of frother is an advantage of reducing the surface tension of water. Bubble radius has a direct relation with the surface tension of water (Young- Laplace, 1805):

$$R_b = \frac{2\gamma}{P_2 - P_1} \quad (5)$$

where γ, R_b, P_1 and P_2 are surface tensions of water, bubble radius, inside pressure of bubble and outside pressure of bubble, respectively. Considering Eqs. 4 and 5, we obtain:

$$\Delta\gamma_{\text{Pine 90}} > \Delta\gamma_{\text{Apirole}} > \Delta\gamma_{\text{A65}} > \Delta\gamma_{MIBC} > \Delta\gamma_{PEB\ 70}. \quad (6)$$

Hence, generation of nano-microbubbles with the smaller size distribution, by Pine 90 compared to the other frothers, was due to the greater reduction in surface tension of water and greater foamability of this frother. Figure 7 shows the effect of frother type on bubble size under identical conditions.

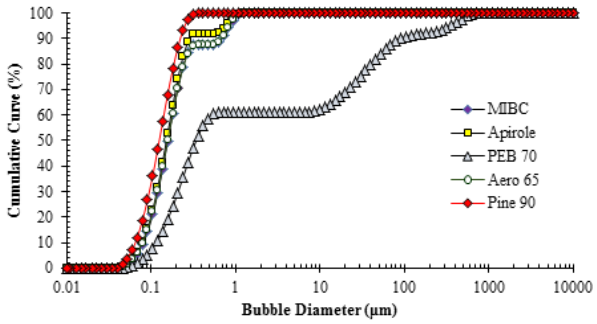

Fig. 7. Frother type effect on bubble size (the same dosage 100 mg/dm^3)

Frother dosage

According to Equation 5 and the proven theory of Young- Laplace, it could clearly be found that increasing frother dosage can cause a further decrease in the surface tension of water and subsequently reduce the bubble size. Figure 8 shows frother dosage effect on the bubble size. Frothers used for this test were Flo-Y-S with two concentrations of 33 and 16 mg/dm^3 and MIBC with two concentrations of 100 and 80 mg/dm^3. As shown in Fig. 8, further increase of frother led to smaller size of bubbles. In addition, low dosage of Flo-Y-S can generate bubbles with diameters smaller than those produced with MIBC. Moreover, the effect of variation of MIBC concentration from 10 to 320 mg/dm^3 as well as Flo-Y-S from 3.3 to 33 mg/ dm^3 on bubble size is shown in Fig. 9.

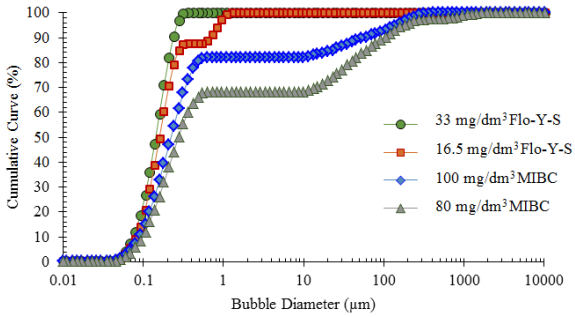

Fig. 8. Effect of frother concentration (comparison of MIBC and Flo-Y-S) on bubble size

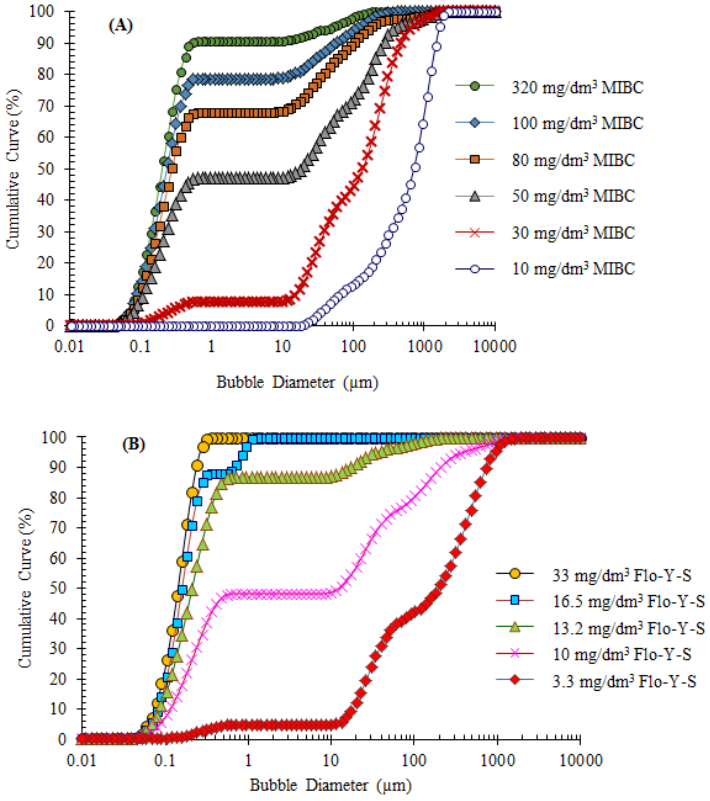

Fig. 9. Effect of a) MIBC and b) Flo-Y-S concentration on bubble size

Increasing the frother concentration could reduce the surface tension and prevent bubble coalescence, which subsequently resulted in bubble size reduction (O'Connor et al., 1989; Comely et al., 2002; Mazahernasab and Ahmadi, 2016). However, there

are some studies suggesting that the bubble size is not particularly controlled by the surface tension. Gupta et al. (2007) studied the relationship between the bubble size and surface tension in the presence of two frothers including MIBC and DF-1012. They demonstrated that when DF-1012 was used as a frother, although the surface tension was lower, the bubble size was larger in comparison to applying MIBC with the same concentration. Moreover, Moyo (2005) showed that adding some salts to the aqueous solution made the bubbles finer, while it increased the surface tension. Azgomi (2006) explained the effect of frother on the bubble size using the bubble coalescence prevention mechanism. He showed that the frother molecules at the air/liquid interface create hydrogen bonds with water and make the liquid film on the bubble surface more stable. Bubble coalescence prevention is expressed based on the frother critical coalescence concentration (CCC) concept, which means that the bubbles are produced in small sizes and frother prevents them from coalescence. Furthermore, Azgomi (2007) suggested that only a part of the bubbles coalescence prevention takes place at CCC and there is another factor having a direct impact on the bubbles size, such as the surface tension.

Dissolved air flow

The air content in the liquid has a significant effect on the occurrence of cavitation. Holl (1970) found that cavitation was directly proportional to the dissolved air content. Increasing the air flow from 0.1 to 0.5 dm^3/min caused the bubble median size to decrease from 323 to 143 nm. Variation of bubble size distribution versus air flow is shown in Fig. 10.

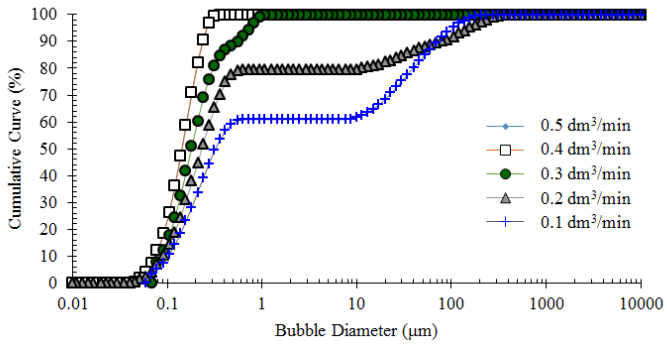

Fig. 10. Effect of dissolved air flow

At a constant temperature, increasing aeration rate, up to a specified amount, will increase the solubility of the air in either water or solution. More dissolution of air in water causes the gradient of dissolved air to reduce at the interface of nanobubbles and environment (water). Thereupon, the air and consequently the pressure inside

nanobubbles remain constant. This causes bubbles to be stable and stay small (Ahmadi et al., 2014).

Inlet pressure to the venturi tube

The variation of inlet pressure to venturi tube is presented in Figure 11. Inlet pressure varied from 150 to 350 kPa. Smaller amounts of bubble diameter occurred at higher values of pressure. The median size of the bubbles (d_{50}) varied from 39.85 μm at 150 kPa to 223 nm at 350 kPa. Obviously, it would be found from the definition of venturi tube that the pressure increment caused a reduction in the velocity of the solution and directly increased the intensity of cavitation, which led to a decrease in the bubbles diameter.

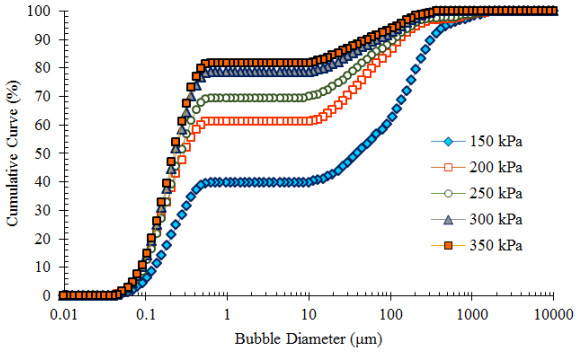

Fig. 11. Effect of pressure variation on bubble size

Pressure has a significant effect on the mean bubble diameter. In general, the mean bubble diameter decreases with increasing pressure, however, above a certain pressure, the bubble size reduction is not significant. The effect of pressure on the mean bubble size is due to changes in the bubble size distribution with pressure. At atmospheric pressure, the bubble size distribution is broad, while under high pressure, the bubble size distribution becomes narrower and is in smaller size ranges. The bubble size is affected by bubble formation at the gas distributor, bubble coalescence and breakup. When the pressure increases the bubble size at the distributor is reduced, bubble coalescence is suppressed, and large bubbles tend to break up, i.e. the maximum stable bubble size is reduced. The combination of these three factors causes the decrease of mean bubble size with increasing pressure (Furusaki, 2001).

Influence of gas type on size distribution of bubbles

Various gases such as filtered compressed air, nitrogen, oxygen, carbone-dioxide and noble gas of argon were applied in this study. Figure 12 shows the bubble size changes as a result of using different gases. As shown, bubbles generated by compressed air and nitrogen are very fine and definitely in the nano range, compared with CO_2 which

generates larger bubble sizes, under the same conditions. This is related to the amount of gas dissolution in water.

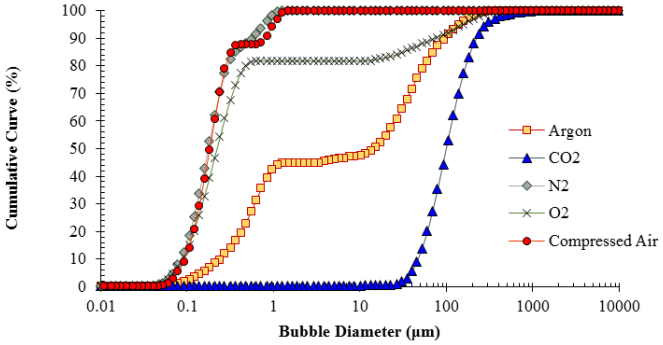

Fig. 12. The effect of gas type variations on bubble size (the same frother concentration, 25 °C, 350 kPa)

The amount of air dissolved in water can be calculated with Henry's law (1803) with the constants at a system temperature of 25 ^{o}C:

oxygen – O_2: 756.7 atm/(mol/dm^3)

nitrogen – N_2: 1600 atm/(mol/ dm^3)

molar weights:

oxygen – O_2: 31.9988 g/mol

nitrogen – N_2: 28.0134 g/mol.

Partial fraction of oxygen and nitrogen in air is about 21 and 79%, respectively. Oxygen and nitrogen dissolved in water at atmospheric pressure can be calculated as:

$$C_O = (1 \text{ atm})\ 0.21 / (756.7 \text{ atm/(mol/dm}^3)) (31.9988 \text{ g/mol}) = 0.0089 \text{ g/dm}^3 \sim 0.0089 \text{ g/kg}$$

$$C_N = (1 \text{ atm})\ 0.79 / (1600 \text{ atm/(mol/dm}^3)) (28.0134 \text{ g/mol}) = 0.0138 \text{ g/dm}^3 \sim 0.0138 \text{ g/kg}.$$

Since air mainly consists of nitrogen and oxygen, the air dissolved in water can be calculated as:

$$C_{Air} = (0.0089 \text{ g/dm}^3) + (0.0138 \text{ g/dm}^3) = 0.0227 \text{ g/dm}^3 \sim 0.023 \text{ g/kg}.$$

Calculating air dissolved in water for some other pressures at a temperature of 25 ^{o}C is summarized in Table 1.

Table 1. Air dissolved in water at various pressures

Pressure, (atm)	1	2	3	4	5	6
dissolved air in water (25 ^{o}C) (g/kg)	0.023	0.045	0.068	0.091	0.114	0.136

The amount of air that can be dissolved in water increases with pressure and decreases with temperature. Solubility (shown by *K*) of other pure gases like carbon dioxide, argon, oxygen and nitrogen in water used in this study for generation of bubbles via cavitation, is shown in Fig. 13. It shows that by increasing the solubility of pure gas in water the median size of the bubbles, which is generated by injection of that gas, increases and vice versa:

$$K_{CO_2} > K_{Ar} > K_{O_2} > K_{Air} > K_{N_2} \tag{7}$$

$$Db(0.5)_{CO_2} > Db(0.5)_{Ar} > Db(0.5)_{O_2} > Db(0.5)_{Air} > Db(0.5)_{N_2}. \tag{8}$$

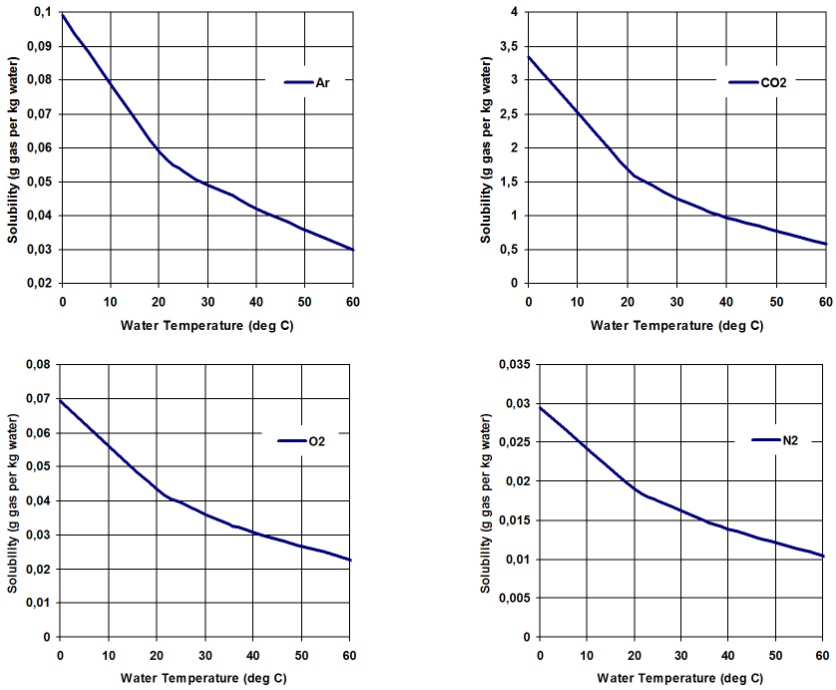

Fig. 13. Solubility of various gases such as argon, carbon dioxide, oxygen and nitrogen in water (Henry, 1803)

Effect of temperature effect on nanobubbles size distribution

If nanobubbles are indeed gas, changes to the temperature of the surrounding environment should change the size and shape of the nanobubbles (Hampton and Nguyen, 2010). Yang et al. (2007) indicated that an increase in the temperature of the hydrophobic surface (25–30 °C) led to the preferential formation of nanobubbles in the vicinity of surface asperities, as shown in Fig. 14. An increase in volume, coalescence and disappearance of those nanobubbles results in a further increase in temperature (up to 40 °C). It is obvious that surface asperities and temperature are important for nanobubble formation. The reason of this phenomenon is not in the

scope of this paper, but Hampton and Nguyen (2010) believed that the possible explanations for this phenomenon included changes in the dynamic stability of nanobubbles and local gas super-saturation. Another possible description is that small pockets of gas are trapped within these rough areas on immersion, which are not visible, and increasing the temperature results in expansion to sizes that are measurable with the AFM (Hampton and Nguyen, 2010).

Yang et al. (2007) also investigated the effect of submerging a hydrophobic surface into waters of different temperatures. It was found that an increase in the temperature of the water increased the nanobubble density. From the AFM images, it appears that the nanobubbles were formed randomly on the surface. Yang et al. (2007) suggested that the rapid heating of the liquid resulted in gas super-saturation, which formed interfacial nanobubbles when exposed to the hydrophobic surface.

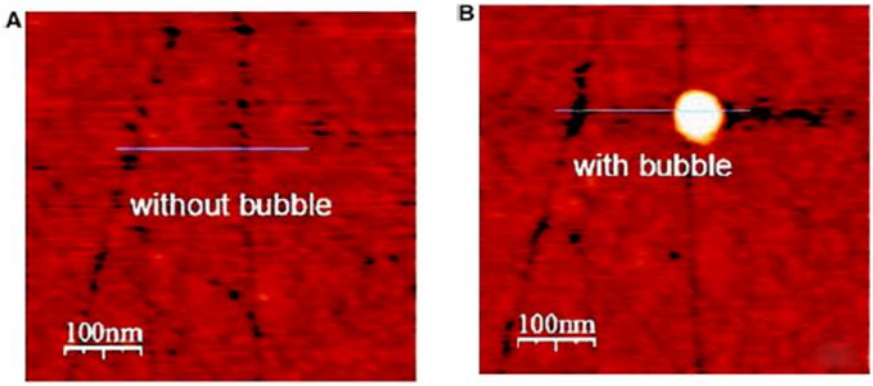

Fig. 14. AFM tapping mode height images of a hydrophobic surface in water at a substrate temperature of: A) 25 °C and B) 30 °C (Yang et al. 2007)

The formation process is similar to the solvent-exchange process. For pre-existing nanobubbles on a hydrophilic mica surface, Zhang et al. (2005) showed that an increase in water temperature from 28 to 42 °C resulted in no significant change of height, however the contact radius increased up to 37 °C, and then decreased. The dependence of gas solubility with temperature was used to explain the results. Zhang et al. (2005) stated that with an increase in temperature, the solubility of the air in the water decreased to a minimum around 37–77 °C. Thus, the nanobubbles grow due to the excess gas in the solution and the size reaches a maximum value where the gas solubility is at a minimum. From Perry's Handbook of Chemical Engineering (Perry et al., 2008), the gas solubility decreases over the temperature range of 0–100 °C.

In this study, the effect of temperature on the nanobubble size distribution was evaluated. For this aim, 100 mg/dm^3 MIBC was used as the frother in the solution at different temperatures. Under the same conditions, temperature of the solution varied. Increasing the temperature from 4 to 60°C resulted in an increase of the median bubble size from 144 to 257 nm (Fig. 15). Thus, it would be found that temperature

increment caused the nanobubbles to generate at a lower velocity of the stream inside the venturi tube. This occurred by increasing the water vapour pressure and decrement of the cavitation number (K_C), based on Eq. (3) (Zhou et al., 1996). Temperature affects the properties of the liquid such as vapour pressure, viscosity, surface tension, gas solubility, and thus affecting the dynamics of the cavity. As temperature increases, vapour pressure increases, while viscosity, surface tension and gas solubility decrease. Since gas solubility is the main source of cavity nuclei, a rise in temperature reduces the gas solubility, and thus reduces the rate of occurrence of cavitation events (Fan and Tao, 2010).

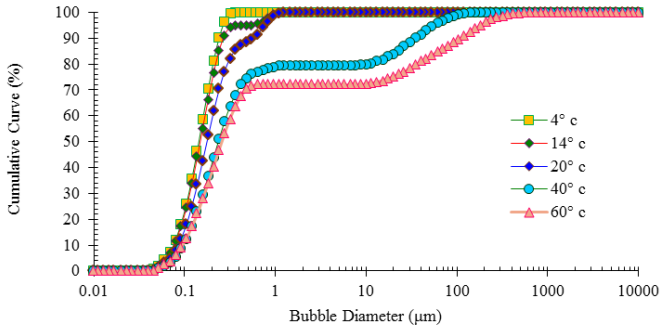

Fig. 15. Influence of temperature on bubble size distribution

pH effect on nanobubble size distribution

In this study, sodium hydroxide and sulphuric acid were used to adjust pH. Moreover, the effect of pH variations on two frother types, MIBC and Flo-Y-S were investigated. As it is observed in Fig. 16, by increasing pH from acidic to alkaline, the median size of bubbles, which are produced by MIBC, was reduced. This is related to the zeta potential of the solutions.

The electrical double layer has an important role in generation and stability of the bubbles in terms of creating the repulsive force (Calgaroto, 2014). Based on the evidence from various studies, the surface of the bubbles generated using MIBC, which is non-ionic frother, in the water has negative charge in a wide range of pH (Elmahdy, 2008). Negativity of the bubble surface charge is due to attraction of OH^- on the bubble surface and the H^+ remaining in the solution because of the differences between the two ions adsorption enthalpy (Wu, 2012). Hydration enthalpy of H^+ and OH^- are equal to -1104 and -446 kJ, respectively (Conway, 1975). Based on Wu et al. (2007), the increment of OH^- concentration has two opposite effects: 1) causes surface charge increment of the bubbles and via electrostatic repulsion force helps the bubbles to be more stable and remain smaller; 2) increases the ionic strength of the solution and removes the effective repulsion force between bubbles. According to Wu et al. (2007), the first reason is more effective and bubbles become finer and more stable at

higher pH. Figure 17 shows the zeta potential variations versus pH in presence of MIBC as a frother.

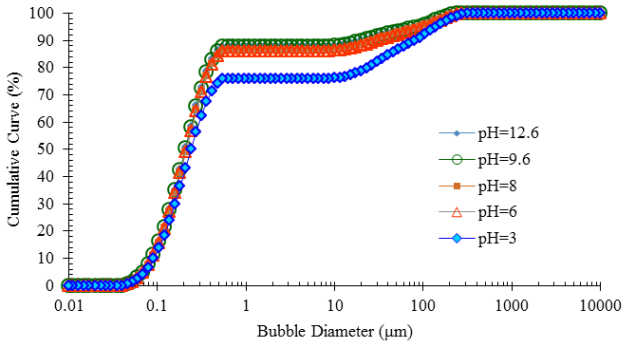

Fig. 16. Influence of pH on size distribution of bubbles (Frother: MIBC 100 mg/dm^3)

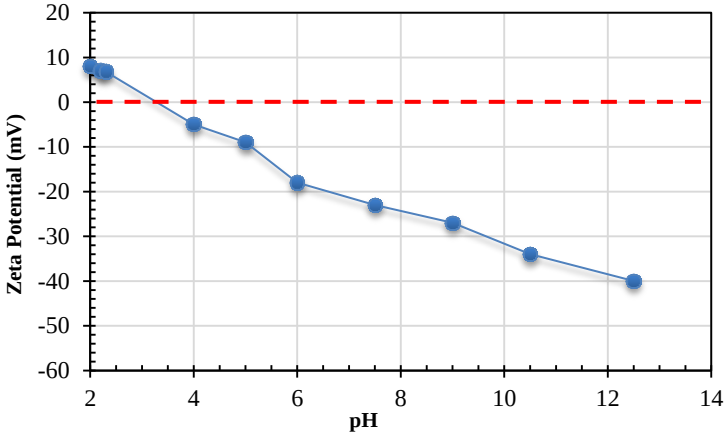

Fig. 17. Zeta potential of bubble in the presence of MIBC 100 mg/dm^3 (Ahmadi, 2014)

Evaluating the zeta potential of Flo-Y-S solution at various pHs showed different results in comparison to MIBC. The bubble charge in the alkaline range was positive and had an incredible increase within pH of 9 to 10, which yielded the same results by repeating the test (Fig. 18). Measurement of the zeta potential in this study was performed by the Micrometrics model 1202 device. An analysis of the bubble size within a pH of 8-9.5, revealed the increasing acidity of Flo-Y-S, which was a kind of fatty acid and anionic surfactant, that caused the bubble size to decrease and conversely, the increment of bubble size was observed by increasing the pH from acidic to alkaline (Fig. 19). Although the procedure of the zeta potential curve was different for nonionic frother of MIBC and anionic frother of Flo-Y-S, but the principle was true for both surfactants. Obviously, by the increment of OH^- concentration due to reducing the pH, the surface charge increment of the bubbles

occurred and the electrostatic repulsion force helped the bubbles to be finer towards higher values of pH.

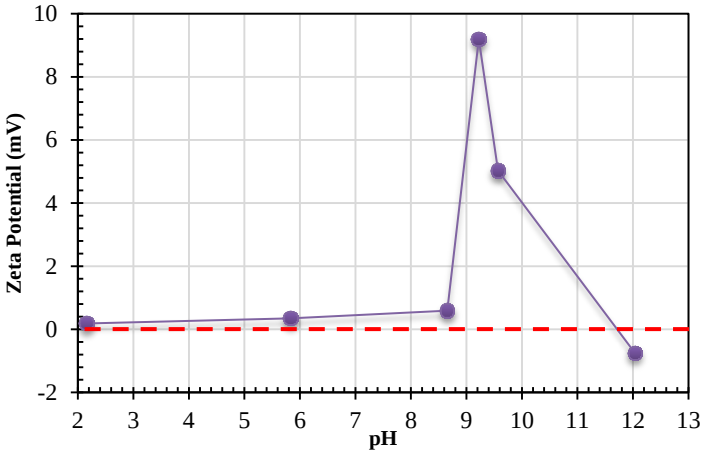

Fig. 18. Zeta potential of bubble in the presence of Flo-Y-S 33mg/dm^3

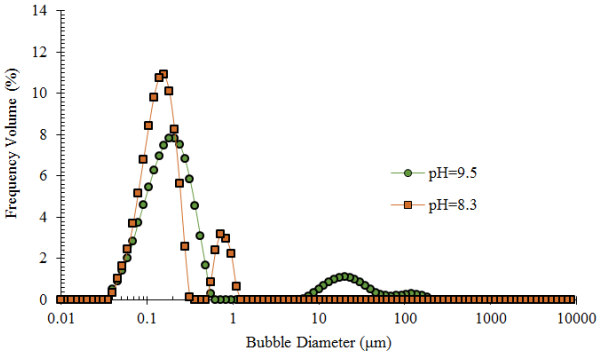

Fig. 19. Influence of pH on size distribution of bubbles (Flo-Y-S 33 mg/dm^3)

Repeatability of results

To evaluate the repeatability of measurement using laser diffraction, 5 measurements were performed under the same conditions of a sample solution containing nano-microbubbles. The coefficient of variation of the measurements was obtained equal to 1.3%. According to the standard ISO 13320 (1999), the coefficient of variation for either particles or bubbles greater than 10 micrometers up to 3% is acceptable in measurements with the laser diffraction method. Based on this standard, for either particles or bubbles finer than 10 micrometers, the coefficient of variation of this value should be doubled (up to 6%). Considering the value of the coefficient of variation obtained in this study, LPSA measurements were reliable and repeatable. Moreover,

the weighted residual of different measurements varied between 0.37 to 0.75%. The residual amount represented the fitness of calculated values (provided model by the software) with the measured values. The residual amount of less than 1% indicates an acceptable fit and residual value greater than 1% shows a lack of right selection in scattering and absorption indices (Ahmadi et al., 2014).

Optimization of effective parameters

The interaction of various parameters on the bubble size was evaluated. For this purpose, the five-level central composite experimental design method was performed for surveying four important parameters affecting the median size and volume of nanobubbles. The specific levels of exclusive variables are demonstrated in Tables 2 and 3. In addition, the analysis of variance is illustrated in Table 4.

Table 2. Levels of variables for a four-factor five-level design of nanobubble generation tests

Variables	Code	Level				
		Low	Middle low	Middle	Middle high	High
		–1.68	–1	0	1	1.68
Frother dosage (mg/dm^3)	A	10	30	50	80	100
pH	B	3	6	8	9.5	12.6
Pressure (kPa)	C	150	200	250	300	350
Air Flow (dm^3/min)	D	0.1	0.2	0.3	0.4	0.5

As observed from Table 3, the model F-value of 157.59 implied that the model was significant. There was only a 0.01% chance that a large model F-value could occur due to noise. Furthermore, values of Prob.> F less than 0.05 indicated that the model terms were significant. In this case A, B, C, AD, CD, A^2, B^2, C^2, A^2B, A^2C, AB^2, AC^2, B^3 are significant model terms.

The lack of fit F-value of 0.27 implied that the lack of fit is not significant relative to the pure error. There is a 96.14% chance that a large lack of fit F-value could occur due to noise. Non-significant lack of fit is good. The statistical analysis of the experimental data gave Eq. (9) for the median size of the cavitation-generated nanobubbles in terms of coded factors:

$$\begin{aligned}\text{Square root } (d_{50} \text{ of bubbles}) = {} & +436.80A + 715.28B - 4.48C - 0.56D \\ & - 2.47AD - 0.98BC + 1.20CD + 90.35A^2 - 4353.43B^2 + 4279.45C^2 - 623.61A^2B \\ & + 2.92A^2C - 21853.77AB^2 + 21403.91AC^2 - 92.16B^3 \end{aligned} \quad (9)$$

where A means the frother dosage, B pH, C the inlet pressure to venturi tube, D is the air flow. Figure 20 shows a normal probability plot of the studentized residuals. The points on this plot lie reasonably on a straight line. The plot does not reveal the above median size model of the cavitation-generated nanobubbles inadequacy. Moreover, Fig. 20 shows the nanobubble size predicted by the above model versus actual

nanobubble size measured in the experiments. The plot indicates that the bubble size model can precisely predict the nanobubble size.

Table 3. Levels of variables for a four-factor five-level design of nanobubble generation tests

Std	Run	Level of Factors			
		A	B	C	D
1	4	–1	–1	–1	–1
2	29	1	–1	–1	–1
3	15	–1	1	–1	–1
4	10	1	1	–1	–1
5	5	–1	–1	1	–1
6	20	1	–1	1	–1
7	23	–1	1	1	–1
8	16	1	1	1	–1
9	3	–1	–1	–1	1
10	25	1	–1	–1	1
11	14	–1	1	–1	1
12	26	1	1	–1	1
13	8	–1	–1	1	1
14	19	1	–1	1	1
15	6	–1	1	1	1
16	12	1	1	1	1
17	22	–1.68	8	0	0
18	7	1.68	8	0	0
19	9	0	–1.68	0	0
20	27	0	1.68	0	0
21	24	0	0	–1.68	0
22	21	0	0	1.68	0
23	18	0	0	0	–1.68
24	1	0	0	0	1.68
25	17	0	0	0	0
26	11	0	0	0	0
27	30	0	0	0	0
28	2	0	0	0	0
29	13	0	0	0	0
30	28	0	0	0	0

Due to the above parameters and obtained responses, the analysis of variance (ANOVA) was conducted with a suitable model to optimize the conditions, with the aim of minimizing the size of air bubbles. Other parameters were maintained in this range. The optimal condition was as follows: frother concentration of 75.8 mg/dm^3, air flow of 0.28 dm^3/min, pressure of 324 kPa and pH of 9.5, in which the d_{50} of bubbles as response was predicted to be 203 nm. These factors were evaluated for MIBC as the frother. To validate the results, a test was performed under optimum conditions. Results showed a good fit at the confidence interval of 95% and reflect the repeatability of the process very well.

Table 4. Analysis of variance table of nanobubble volume
for four-factor five-level central composite experiments

Source	Sum of squares ($\times 10^{-3}$)	df	Mean square	F Value	*p*-value Prob> F
Model	10645.79	15	709.72	157.59	< 0.0001
A-Frother Dosage	114.45	1	114.45	25.41	0.0001
B-pH	160.91	1	160.91	35.73	< 0.0001
C-Pressure	146.25	1	146.25	32.47	< 0.0001
D-Air Flow	7.60	1	7.60	1.69	0.2134
AD	99.25	1	99.25	22.04	0.0003
BC	15.22	1	15.22	3.38	0.0859
CD	22.99	1	22.99	5.10	0.0392
A^2	169.72	1	169.72	37.69	< 0.0001
B^2	119.35	1	119.35	26.50	0.0001
C^2	119.35	1	119.35	26.50	0.0001
A^2B	161.16	1	161.16	35.78	< 0.0001
A^2C	41.58	1	41.58	9.23	0.0083
AB^2	119.44	1	119.44	26.52	0.0001
AC^2	119.40	1	119.40	26.51	0.0001
B^3	161.91	1	161.91	35.95	< 0.0001

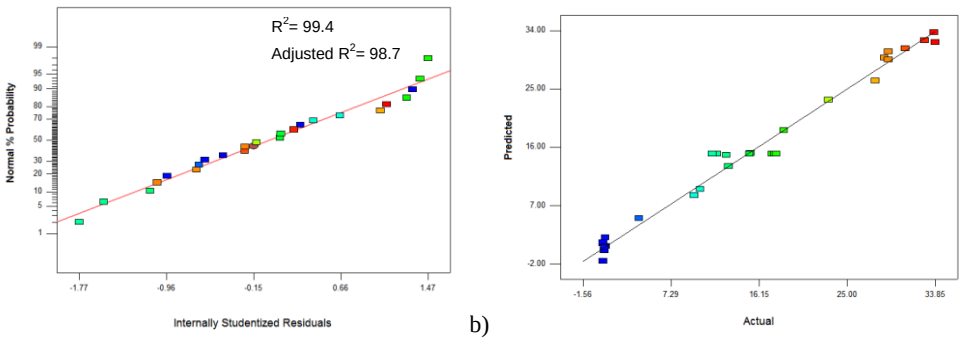

Fig. 20. Normal probability plot of studentized residuals (a), and predicted nanobubble size versus actual nanobubble size (b)

Conclusions

1) Nanobubble sizes decreased as the frother concentration increased. At the particular values of the other six studied parameters, the median nanobubble size decreased from 197 μm to 143 nm when Flo-Y-S concentration increased from 3 to 33 mg/dm^3. The same trend occurred, but with larger bubble size, when MIBC was used as a frother.

2) Generated nanobubbles by Flo-Y-S as a frother were significantly smaller than the bubbles in the presence of MIBC.
3) Nanobubble sizes increased with increasing the dissolved air flow rate. At the particular values of the other six studied parameters, nanobubble sizes varied from 323 to 143 nm with increasing dissolved air flow rate from 0.1 to 0.5 dm^3/min.
4) The median size of the nanobubbles constantly increased with increasing the time interval.
5) The size of the nanobubbles decreased with increasing the pressure within the nanobubble generator. At the particular values of the other six studied parameters, the median bubble size decreased from 39.8 μm to 223 nm as the pressure increased from 150 to 350 kPa.
6) The pH effect was surprisingly different for different frothers. The median size of the nanobubbles increased with decreasing pH from basic to acidic values by using MIBC. At the particular values of the other six studied parameters by varying pH from 12.63 to 3.13, the median size of nanobubbles changed from 207 to 240 nm for MIBC and this trend was reversed for Flo-Y-S, so that at the particular values of the other six studied parameters, the median nanobubble size decreased from 209 to 158 nm as the pH changed from 9.5 to 8.
7) The venturi tube internal diameter had a significant influence on the size of the bubbles. Thus, the median size of the bubbles at the specific values of the other six studied parameters was changed from 13 μm to 223 nm for the venturi diameter of 2.2 and 1.5 mm, respectively.
8) With the aim of minimizing the size of air bubbles, according to analysis of variance, the optimal condition was as follows: frother concentration 75.8×10^{-6}, air flow 0.28 dm^3/min, pressure 324 kPa and pH 9.5, in which d_{50} of bubbles, as response, was predicted to be 203 nm. These factors were evaluated for MIBC as the frother. For validating the results, a test was performed under optimum conditions. Results showed a good fit at the confidence interval of 95% and reflected the repeatability of the process.

Acknowledgements

This research project is supported by Iran Mineral Processing Research Center. Hereby, the authors wish to acknowledge the IMPRC and Iranian Mines and Mining Industries Development and Renovation Organization (IMIDRO) for their financial support.

References

AHMADI R., KHODADADI DARBAN, A., 2013, *Modelling and optimization of nano-bubble generation process using response surface methodology*, International Journal of Nanoscience and Nanotechnology, Vol. 9, No. 3, 151-162.

AZGOMI F., 2006, *Characterizing frothers by their bubble size control properties*, Master Thesis in Metals and Materials Engineering, McGill University, Montreal, Canada.

AZGOMI, F., GOMEZ, C.O., FINCH, J.A., 2007, *Correspondence of gas holdup and bubble size in presence of different frothers*, International Journal of Mineral Processing, 83, 1–11.

CALGAROTO S., WILBERG K.Q., RUBIO J., 2014, *On the nanobubbles interfacial properties and future applications in flotation*, Minerals Engineering, 60, 33-40.

CONWAY B.E.,1975, *Ion hydration near air/water interfaces and the structure of liquid surfaces*, Journal of Electroanalytical Chemistry, 65, 491-504.

ELMAHDI A.M., MIRNEZAMI M., 2008, FINCH J.A., *Zeta potential of air bubbles in presence of Frothers*, International Journal of Mineral Processing, 89, 40–43.

FAN M., TAO D., 2008, *A study on picobubble enhanced coarse phosphate froth flotation*, Separation Science and Technology, 43, 1-10.

FAN M., 2008, *Picobubble enhanced flotation of coarse phosphate particles*, Ph.D. Dissertation in Mineral Processing, University of Kentucky, Kentucky, USA.

FAN M., TAO D., HONAKER, R., LUO, Z., 2010, *Nanobubble generation and its application in froth flotation (part I): nanobubble generation and its effects on properties of microbubble and millimetre scale bubble solutions*, Mining Science and Technology 20, 1–19.

FAN M., TAO D., HONAKER, R., LUO, Z., 2010, *Nanobubble generation and its applications in froth flotation (part II): fundamental study and theoretical analysis*, Mining Science and Technology, 20, 159-177.

FURUSAKI S., 2001, *The expanding world of chemical engineering*. CRC Press,175-176.

ISO 13320, 2009, *Particle size analysis-laser diffraction methods*, Part 1, General principals.

GUPTA A.K., BANERJEE P.K., MISHRA A., SATISH P., 2007, *Effect of alcohol and polyglycol ether frothers on foam stability, bubble size and coal flotation*, International Journal of Mineral Processing, 82, 126– 137.

LI S.C., 2001, *In cavitation of hydraulic machinery*, ICP, London, Chapters 7 and 8.

HAMPTON M.A., NGUYEN A.V., 2010, *Nanobubbles and the nanobubble bridging capillary force*, Advances in Colloid and Interface Science, 154, 30–55.

HENRY W., 1803, *Experiments on the quantity of gases absorbed by water, at different temperatures, and under different pressures*. Philosophical Transactions of the Royal Society of London 93, 29–274.

HOLL J. W., 1970, *Nuclei and cavitation*, Journal of Basic Engineering 92.4 ,681-688.

JIN F., LI J., YE X., WU Ch., 2007, *Effects of pH and ionic strength on the stability of nanobubbles in aqueous solutions of cyclodextrin*, Journal of Physical Chemistry, 111, 11745-11749.

MAZAHERNASAD R., AHMADI R., 2016, *Determination of bubble size distribution in a laboratory mechanical flotation cell by a laser diffraction technique*, Physicochemical Problems of Mineral Processing, 52, 690-702.

MOYO P., 2005, *Characterization of frothers by water carrying rate*, Doctoral Dissertation in Metals and Materials Engineering, McGill University, Montreal, Canada.

OCONNOR C.T., RANDALL E.W., GOODALL C.M., 1989, *Measurement of the effects of physical and chemical variables on bubble size*, International Journal of Mineral Processing, 28, 139-149.

PERRY R.H., GREEN D.W., ACKERS D.E., 2008, *Perry's chemical engineers' handbook*, McGraw-Hill.

LAPLACE P.S., 1805, *Supplement to the tenth book of the "Traite de Mecanique Celeste",* (in French), Vol. 4, Paris, France, Courcier, 1-79.

SAYADI H., 2007, *Unsteady flow cavity in the water treatment reactors*, Ph.D. Dissertation (in Persian), University of Khajeh Nasiroddin Toosi,Tehran, Iran.

SOBHY A., TAO D., 2013, *Nanobubble column flotation of fine coal particles and associated fundamentals*, International Journal of Mineral Processing 124, 109-116.

TAO D., 2004, *Role of bubble size in flotation of coarse and fine particles-a review*, Separation Science and Technology, 39, 741-760.

WU Ch., NESSET K., MASLIYAH J., XU Zh., 2012, *Generation and characterization of submicron size bubbles*, Advances in Colloid and Interface Science, 19, 123–132.

YANG S., DAMMER S.M., BERMOND N., ZANDVLIET H.J.W., KOOIJ E.S. S., LOHSE D., 2007, *Characterization of Nanobubbles on Hydrophobic Surfaces in Water*, Langmuir, Vol. 23, 7072-7073.

YOUNG T., 1805, *An essay on the cohesion of fluids,* Philosophical Transactions of the Royal Society of London, ,95, 65–87.

ZHANG M, SEDDON J.R., 2016, *Nanobubble–nanoparticle interactions in bulk solutions,* Langmuir 32, No. 43, 11280-11286.

ZHANG X.H., LI G., WU Z.H., ZHANG X.D., HU J., 2005, *Effect of temperature on the morphology of nanobubbles at mica/water interface*, Chinese Physics, 14 (9).

ZHANG X.H., MAEDA N., CRAIG V.S.J., 2006, *Physical properties of nanobubbles on hydrophobic surfaces in water and aqueous solutions*, Langmuir, Vol.22, 5025-5035.

ZHOU Z.A., XU Z.H., FINCH J.A., MASLIYAH J.H., CHOW R.S., 2009, *On the role of cavitation in particle collection in flotation-a critical review II*, Minerals Engineering, 22, 419-433.

ZHOU Z.A., ZHENGHE X.U., FINCH J.A., 1994, *On the role of cavitation in particle collection during flotation- A critical review*, Minerals Engineering, 7(9), 1073-1084.